



Dryness/wetness variations in ten large river basins of China during the first 50 years of the 21st century

Jian Qing Zhai^b, Bo Liu^{a,b,*}, Heike Hartmann^c, Bu Da Su^b, Tong Jiang^b, Klaus Fraedrich^d

^a Department of Water Resources and Hydrology, Hohai University, Nanjing 210024, China

^b National Climate Center, China Meteorological Administration, Beijing, 100081, China

^c Department of Geography, Justus Liebig University, Giessen, Germany

^d Meteorological Institute, Hamburg University, Hamburg, Germany

ARTICLE INFO

Article history:

Available online 12 February 2010

ABSTRACT

This study investigated future changes of dryness/wetness in ten large river basins: the Songhuajiang River basin, the Liaohe River basin, the Haihe River basin, the Yellow River basin, the Huaihe River basin, the Yangtze River basin, the Pearl River basin, the Southeast River basins, the Southwest River basins and the Northwest Inland River basins across China during the first 50 years of the 21st century. The study was carried out according to the Standardized Precipitation Index (SPI), which is calculated by monthly precipitation data of ECHAM5/MPI-OM. Three anthropogenic greenhouse gas emission scenarios, SRES-A2, SRES-A1B and SRES-B1 have been considered. The frequency of dry/wet periods in these river basins was calculated and the trend detected by the Mann–Kendall non-parametric test. The results reveal that there is a trend towards drier conditions from northeast to southwest China in scenario A2 and a similar spatial distribution pattern in scenario A1B and B1. Areas with a high frequency of drought are detected under all three scenarios. In the next half century, the Haihe River basin, northeast China, is expected to show a significant trend towards drier conditions, which pass the 95% confidence level in scenario A2. In the Yellow River basin, the Huaihe River basin, the Yangtze River basin and the Pearl River basin, an obvious trend towards wetter conditions has been detected in scenario A1B. The Songhuajiang River basin, the Haihe River basin, the Yellow River basin and the Huaihe River basin show a trend towards wetter conditions, which passed the 90% confidence level in scenario B1. The future dryness/wetness frequency situation is complex in the ten large river basins.

© 2010 Elsevier Ltd and INQUA. All rights reserved.

1. Introduction

Global warming is unequivocal, as is now evident from observations of increases in global average air temperature. There is also observational evidence from all continents and most oceans that many natural systems are affected by regional climate changes (IPCC, 2007). It is one of the most important frontier fields of presently global change research to study the changing characteristics of regional climate. Drought is one of the major natural hazards that bring about billions of dollars in loss to the agricultural community of the world every year (Narasimhan and Srinivasan, 2005; Su et al., 2007). Bordi and Sutera (2002) presented a study

on the drought occurrence in Italy based on the NCEP/NCAR reanalysis precipitation rates covering the period from 1948 to 2000. They implied that drought conditions have been more frequent and extended in the recent past. Li et al. (2004) analyzed the change trend of the Palmer Drought Severity Index (PDSI) and the possible response of the drought change rate to global warming in the main arid regions of the world for the recent hundred-odd years by global grids of $2.5^\circ \times 2.5^\circ$. The results showed that there is an obvious trend towards drier conditions in the main arid regions of South America, South Africa, North America, Central Asia and northwest China.

It is also important to analyze the variation of dryness/wetness in China. Many studies have been conducted regarding climate drought in China in the past years. Li et al. (1996) drew a conclusion that there were four large drought centers in China and there was a linear tendency of drying in the whole country. Zhai and Zou (2005) analyzed the characteristics of drought in China during 1951–2003 according to the data of 606 meteorological stations.

* Corresponding author at: Hohai University, 1# Xikang Road, Nanjing 210024, China. Tel.: +86 025 83787491.

E-mail addresses: jianqing9801@163.com (J.Q. Zhai), bobol3705@163.com (B. Liu), heike.hartmann@geogr.uni-giessen.de (H. Hartmann), subd@cma.gov.cn (B. Da Su), jiangtong@cma.gov.cn (T. Jiang).

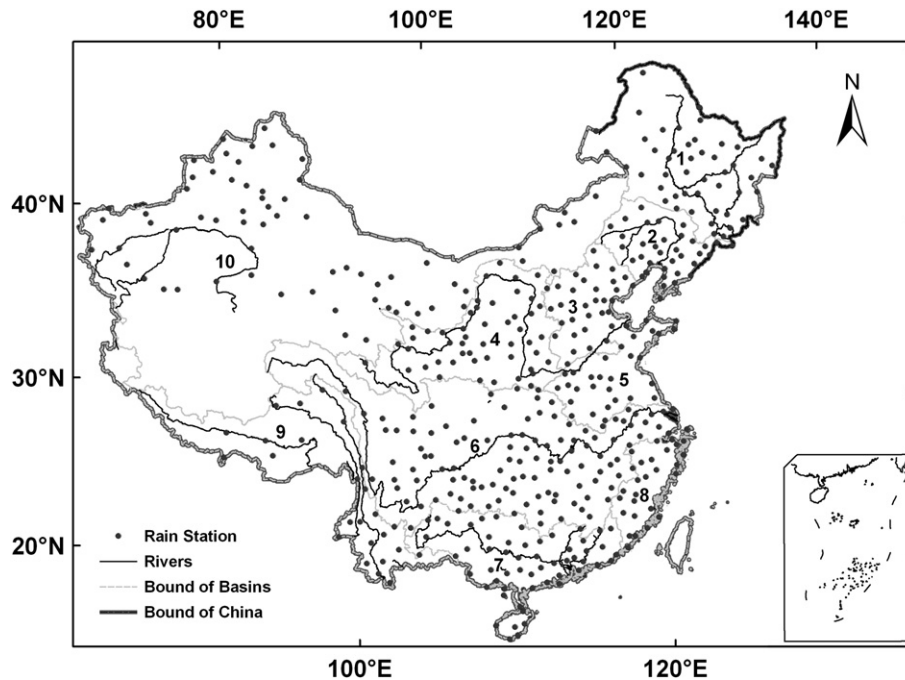


Fig. 1. Ten large river basins in China. (Numbers denote the ten river basins: 1, the Songhuajiang River basin; 2, the Liaohe River basin; 3, the Haihe River basin; 4, the Yellow River basin; 5, the Huaihe River basin; 6, the Yangtze River basin; 7, the Pearl River basin; 8, the Southeast River basins; 9, the Southwest River basins; 10, the Northwest Inland River basins.)

They pointed out that precipitation was the most important factor for drought changes. In the past 50 years, there is an insignificant increasing trend for drought areas. Ma and Ren (2007) analyzed the relationship between climate change and trend towards drier conditions based on the monthly mean surface air temperature and monthly precipitation data of 160 meteorological stations over China from 1951 to 2006. They found that there were drier trends in North China, Northeast China, the east part of Northwest China, and Southwest China. Phase and duration of the drying processes were different in the above mentioned regions. Many other researchers detected a drier trend in North China and Northeast China in the past 50 years (Zhang, 1998; Wang and Zhai, 2003; Xie et al., 2003; Bordi et al., 2004; Wei, 2004). All of these studies concentrate on the variation of dryness/wetness in the past. The present study is an objective dryness/wetness assessment of China during the first 50 years of the 21st century.

The aim of this study is to apply the Standardized Precipitation Index (SPI) in order to identify dryness/wetness periods during the first 50 years of the 21st century in China. Data and analytical methods used in this study are described in Section 2. In Section 3 the simulation capability of the ECHAM5 model is tested on annual averaged precipitation scale. The results of calculated SPI derived from the monthly precipitation data of the three scenarios of ECHAM5/MPI-OM and the analysis of dryness/wetness in China is

shown in Section 4. Discussion and conclusions are presented in Section 5. This study will help to understand variations of water resources in the next 50 years of the 21st century in China.

2. Study area, data and methods

2.1. Study area and data

China consists of ten large river basins: the Songhuajiang River basin, the Liaohe River basin, the Haihe River basin, the Yellow River basin, the Huaihe River basin, the Yangtze River basin, the Pearl River basin, the Southeast River basins, the Southwest River basins and the Northwest Inland River basins (Fig. 1). Because China has a vast territory and complicated terrain, its climate has significant diversity. Annual averaged precipitation gradually decreases from southeast China to northwest China. Due to the uneven distribution of precipitation, not only in different regions but also in different seasons, droughts and floods frequently occur.

Data from 752 meteorological stations in China were provided by the National Climate Center of the China Meteorological Administration. In this study, only 483 stations were chosen after being checked by the following criteria: data quality, continuity, homogeneity and the length of data record. All these stations have uninterrupted observational monthly precipitation data from 1961 to 2007. Periods during 1961–2000 were chosen for testing and verifying the simulation ability of the ECHAM5 model. Monthly precipitation data (2001.01–2050.12) of three scenarios (SRES-A2, SRES-A1B and SRES-B1) from simulations of the GCM ECHAM5/MPI-OM were used for the calculation of SPI. This paper is mainly focused on the basic variation characters of dryness/wetness in the future in China, so SPI was calculated based on the averaged results of the 3 runs for the A1B and B1 scenarios, and of the 4 runs for the A2 scenario. The scenarios were explained by IPCC in 2000 (IPCC, 2001) for use in the Third Assessment Report (Nakicenovic and Swart, 2000). Scenario A2 represents a very heterogeneous world with continuously increasing global population and regionally

Table 1
Categorization of the dryness/wetness grade by the SPI.

Categories	SPI values
Extremely dryness	≤ -2.0
Severe dryness	-1.99 to -1.5
Moderate dryness	-1.49 to -1.0
Near normal	-1.0 to 1.0
Moderate wetness	1.0–1.49
Severe wetness	1.5–1.99
Extremely wetness	≥ 2.0

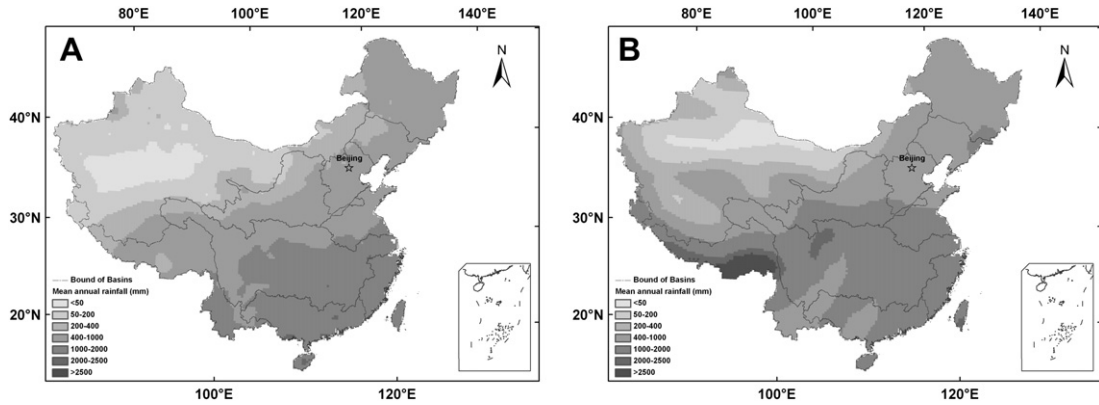


Fig. 2. Spatial distribution of mean annual rainfall during 1961–2000. (A: data from 483 observational meteorological stations; B: data from ECHAM5 model.)

oriented economic growth that is more fragmented than in other scenarios; B1 represents a convergent world with rapid global population growth but with rapid changes in economic structures towards a service and information economy, with reductions in material intensity and the introduction of clean and resource-efficient technologies; A1B represents a situation which is between the A2 and B1 scenarios (Nakicenovic and Swart, 2000). The ECHAM5 data were provided by the Max Planck Institute for Meteorology (MPIM). The resolution of the atmospheric model ECHAM5 is triangular T63 ($1.875^\circ \times 1.875^\circ$) with 31 vertical levels. The atmospheric model is coupled with the ocean model MPI-OM with 1.5° resolution without flux correlation (Blender and Fraedrich, 2006).

2.2. Drought indices

Drought is a complex phenomenon that mostly describes a persistent deficit of precipitation in a particular area. Dracup et al. (1980) classify drought into three categories: meteorological, agricultural, and hydrological drought. Meteorological drought is defined by a period of substantially diminished precipitation in both duration and intensity. In general, indices of drought are based on precipitation amount and they may differ in other climatological parameters (such as temperature, pressure, evapotranspiration and soil moisture) that could be taken into account (Bordi and Sutera, 2002). There are many drought indices, such as the Palmer Drought Severity Index (PDSI), which has been widely used. Compared with PDSI, the SPI is derived from precipitation alone to represent water deficit and surplus, and can be easily computed. As well, the index is standardized, so it is suitable for comparing different regions or watersheds (Bordi et al., 2004). The SPI was

developed by McKee et al. (1993) for the identification of dry/wet periods and to evaluate their severity (Moreira et al., 2006). Up to now, the SPI has been used for drought monitoring in Colorado, United States (McKee et al., 1993), for analyzing droughts in Western Iran (Raziei et al., 2009), for drought monitoring over Africa (Barbosa et al., 2009), and for assessing regional drought in the Marche region, Italy (Bordi et al., 2001). The SPI can be calculated for shorter or longer time scales, which may reflect lags in the response of different water resources to precipitation anomalies (Paulo et al., 2003). Originally, the SPI was calculated for 3-, 6-, 12-, 24- and 48-month time scales (McKee et al., 1993). A 3-month SPI reflects short and medium term moisture conditions and provides a seasonal estimation of precipitation, comparing the precipitation over a specific 3-month period with the precipitation totals from the same 3-month period for all the years included in the historical record (Tsakiris and Vangelis, 2004). As the time scale increases, the SPI responds more slowly to changes in precipitation, and results for the 12-month time scale identify dry periods of long duration, which relate with the global impact of drought on hydrologic regimes and water resources of a region (Moreira et al., 2008). Due to this reason, in this study the 12-month time scale has been selected.

There are two algorithms used for calculating SPI. One method is described by McKee et al. (1993), which assumes a random variable following a Pearson distribution Type III. The other one to compute the SPI, which is applied in this study, is described by Bordi and Sutera (2002) as follows. If x is the random variable, the gamma distribution is defined by its probability density function as

$$g(x) = \frac{1}{\beta^\alpha \tau(\alpha)} x^{\alpha-1} e^{-x/\beta} \quad \text{for } x > 0,$$

where $\alpha > 0$ is a shape parameter, $\beta > 0$ is a scale parameter and $\tau(\alpha)$ is the gamma-function.

Also:

$$\tilde{\alpha} = \frac{1}{4A} \left(1 + \sqrt{1 + \frac{4A}{3}} \right), \quad \tilde{\beta} = \frac{\bar{x}}{\tilde{\alpha}},$$

where

$$A = \ln(\bar{x}) - \frac{\sum \ln(x)}{n},$$

where n is the number of observations in which some precipitation has occurred. \bar{x} , given a particular month, is the mean of the cumulative precipitation computed for the same month for the different years in the record.

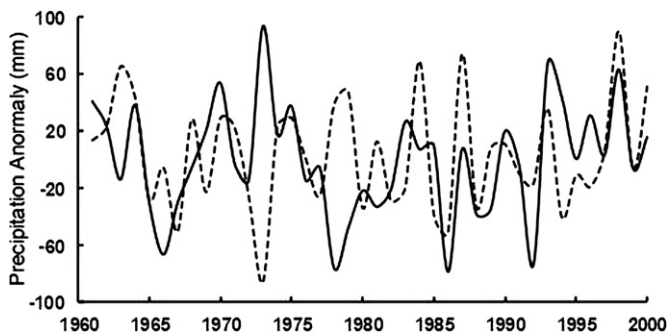


Fig. 3. Precipitation anomaly during 1961–2000 in China. (Dark line: precipitation from observational meteorological station; dotted line: precipitation from ECHAM5 model.)

Table 2
Comparison of seasonal precipitations in China during 1961–2000 (mm).

Season	Category	Observed data	Simulated data	Difference
Spring	Average value	211.8	243.0	31.2
	Stan. devi.	22.8	18.3	–4.5
Summer	Average value	413.8	356.5	–57.3
	Stan. devi.	31.1	26.5	–4.7
Autumn	Average value	166.0	141.9	–24.2
	Stan. devi.	23.5	21.5	–2.1
Winter	Average value	60.6	81.1	20.6
	Stan. devi.	16.2	13.6	–2.6
Year	Average value	852.2	822.5	–29.7
	Stan. devi.	47.7	38.8	–8.9

The cumulative probability, letting $t = x/\bar{\beta}$, becomes the incomplete gamma-function:

$$G(x) = \int_0^x g(x) dx = \frac{1}{\tau(\tilde{\alpha})} \int_0^x t^{\tilde{\alpha}-1} e^{-t} dt.$$

Since the gamma-function is undefined for $x=0$ and the precipitation field may contain zeros, the cumulative probability becomes

$$H(x) = q + (1 - q)G(x),$$

where q is the probability of zero precipitation.

$H(x)$ is then transformed to a normalized variable Z by means of the following approximation:

$$Z = \text{SPI} = -\left(t - \frac{c_0 + c_1 t + c_2 t^2}{1 + d_1 t + d_2 t^2 + d_3 t^3}\right), \quad \text{for } 0 < H(x) \leq 0.5,$$

$$Z = \text{SPI} = +\left(t - \frac{c_0 + c_1 t + c_2 t^2}{1 + d_1 t + d_2 t^2 + d_3 t^3}\right), \quad \text{for } 0.5 < H(x) < 1,$$

where

$$t = \sqrt{\ln\left(\frac{1}{(H(x))^2}\right)}, \quad \text{for } 0 < H(x) \leq 0.5,$$

$$t = \sqrt{\ln\left(\frac{1}{(1.0 - H(x))^2}\right)}, \quad \text{for } 0.5 < H(x) < 1.0,$$

and $c_0, c_1, c_2, d_1, d_2, d_3$ are the following constants:

$$c_0 = 2.515517, \quad d_1 = 1.432788,$$

$$c_1 = 0.802853, \quad d_2 = 0.189269,$$

$$c_2 = 0.010328, \quad d_3 = 0.001308.$$

Table 3
Comparison of observed and simulated annual precipitations in ten large river basins in China during 1961–2000.

River basins	Songhuajiang River basin	Liaohu River basin	Haihe River basin	Yellow River basin	Huaihe River basin	Yangtze River basin	Pearl River basin	Southeast River basins	Southwest River basins	Northwest River basins
Correlation coefficient	0.80	0.72	0.67	0.59	0.59	0.57	0.64	0.15	0.17	0.5

So, the SPI represents a Z-score or the number of standard deviations that an event deviates from the mean. The classification of dry and wet events intensities resulting from SPI computation is shown in Table 1.

SPI is based on the long-term precipitation record for a selected location and is a meteorological index (Krysanova et al., 2008), so the analyses in this paper are mainly focused on meteorological drought.

2.3. Trend analysis methods

The trend tests applied in this study are the non-parametric Mann–Kendall test, which is a rank-based procedure suitable for detecting non-linear trends. More details can be found in previous studies (Mann, 1945; Kendall, 1975; Wilks, 1995; von Storch and Zwiers, 1999).

The Mann–Kendall method, as described in Zhang et al. (2005), assumes that the time series is $x_1, x_2, x_3, \dots, x_n$, and m_i denotes the cumulative total of samples so that $x_i > x_j$ ($1 \leq j \leq i$), where n is the number of the sample.

The definition of the statistical parameter d_k is as follows:

$$d_k = \sum_i^k m_i \quad (2 \leq k \leq N),$$

on the condition that the original time series was random and independent. The variance and mean of d_k are defined as:

$$E[d_k] = \frac{k(k-1)}{4},$$

and

$$\text{var}[d_k] = \frac{k(k-1)(2k+5)}{72} \quad 2 \leq k \leq N.$$

Under the assumption above, the definition of statistical index of UF_k is as follows:

$$UF_k = \frac{d_k - E[d_k]}{\sqrt{\text{var}[d_k]}} \quad (k = 1, 2, 3, \dots, n).$$

Confidence probability of 90%, 95% and 99% is considered to be significant and discussed respectively later. The trends of dryness/wetness were spatially interpolated by applying the inverse distance weighted (IDW) interpolation method.

3. Test of the precipitation simulation ability of the ECHAM5 model in China

The annual averaged precipitation and precipitation anomalies are calculated based on observational monthly precipitation derived from 483 meteorological stations as well as monthly rainfall simulated by ECHAM5 model in China during 1961–2000. The results indicate that there is a decreasing trend from southeast China to northwest China with annual precipitation ranges from over 2000 mm to less than 50 mm both for observational and simulated annual averaged precipitation, although the magnitude of the simulated mean annual precipitation is larger than that of the

observational rainfall (Fig. 2). Precipitation anomalies also indicate that the annual trend is different before 1980 but is in good agreement between observational precipitation and projected rainfall during 1980–2000 (Fig. 3). There is an obvious mutation of atmosphere and ocean circulation of the northern hemisphere during the 1970s, but the ECHAM5 model does not capture this change, so a discrepancy exists (Sun and Ding, 2008).

Seasonal precipitations are compared between observed and simulated rainfall during 1961–2000 in China, listed in Table 2. This table shows that precipitations of spring and winter derived from ECHAM5 model are higher than observed values, yet are lower in summer and autumn. The precipitation is more similar in autumn and winter, with standard deviation values of only –2.1 and –2.6 respectively between simulated and observed data.

This study computes the correlation coefficient of annual precipitations between observed and simulated data in ten large river basins in China during the 1961–2000 (Table 3). It shows that the simulation capability of the model is acceptable in most of river basins in China, except in the Southeast River basins and South River basins, with coefficient values of 0.15 and 0.17.

In all, the ECHAM5 model can generally simulate the precipitation pattern in China although there is some uncertainty in some regions and times. As a GCM model, the above research confirms that it is reliable to some extent to project the character of future dryness/wetness variations based on the ECHAM5 model in China.

4. Results

4.1. Spatial distribution of dryness/wetness

The number of dry months with the SPI values < –1 in grid box, which has been classified as the dry months using the SPI as the drought metric, is counted for the three scenarios for the first 50 years of the 21st century. In the A2 scenario, one high value area

exists in North China during 2002–2050. This region includes the Songhuajiang River basin, the north part of the Liaohe and Yellow River basins, and some areas of the Northwest River basins. In addition, two high value centers are located in the Jinshajiang River catchment and the Hanjiang River catchment. There are two high value areas with many dry months in the eastern part of the Huaihe River basin and the south part of the Pearl River basin (Fig. 4a). Fig. 4b shows that other high value areas are located in the Songhuajiang River basin, the south part of Yellow River basin, the Jinshajiang River catchment, the Pearl River basin, the Southwest River basins and some parts of Northwest River basins in the A1B scenario. In the B1 scenario, the areas with high frequency of dryness may include the Haihe River basin, the east part of Yellow River basin, the Dongting lake catchment of the Yangtze River basin, the Southeast River basins and some parts of Northwest River basins (Fig. 4c).

4.2. Trend analysis of dryness/wetness

The spatial distribution of the Mann–Kendall (MK) trend statistic of every grid cell is shown in Fig. 5. The positive and negative trends, which represent trends towards wetter and drier conditions, are detected.

It is known from the MK trends of the SPI index that in the A2 scenario (Fig. 5a) there is a negative trend from northeast to southwest China which covers the Songhuajiang River basin, the Liaohe River basin, the Haihe River basin, the Yellow River basin, the Upper reaches of the Yangtze River basin and the west part of Pearl River basin. Positive trends dominate in the northwest and the southeast of China, including the northwest parts of the Inland River basins, the middle and lower Yangtze River basin and west of Qinghai-Tibet Plateau which covers part of the Southeast River basins (Fig. 5a). This situation is similar with the observational trend during 1961–2005. Fig. 5b indicates wetness/doughtiness

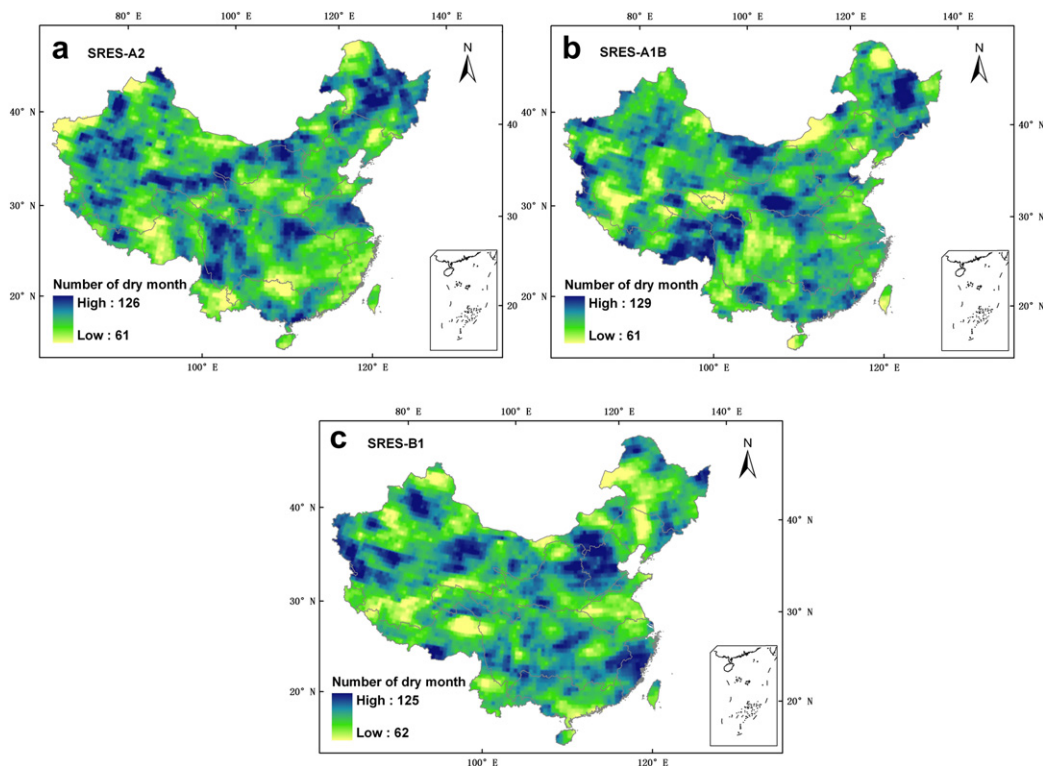


Fig. 4. The number of all dry months during 2002–2050 (588 months) (a) scenario A2, (b) scenario A1B, (c) scenario B2 (letter denotation the same below).

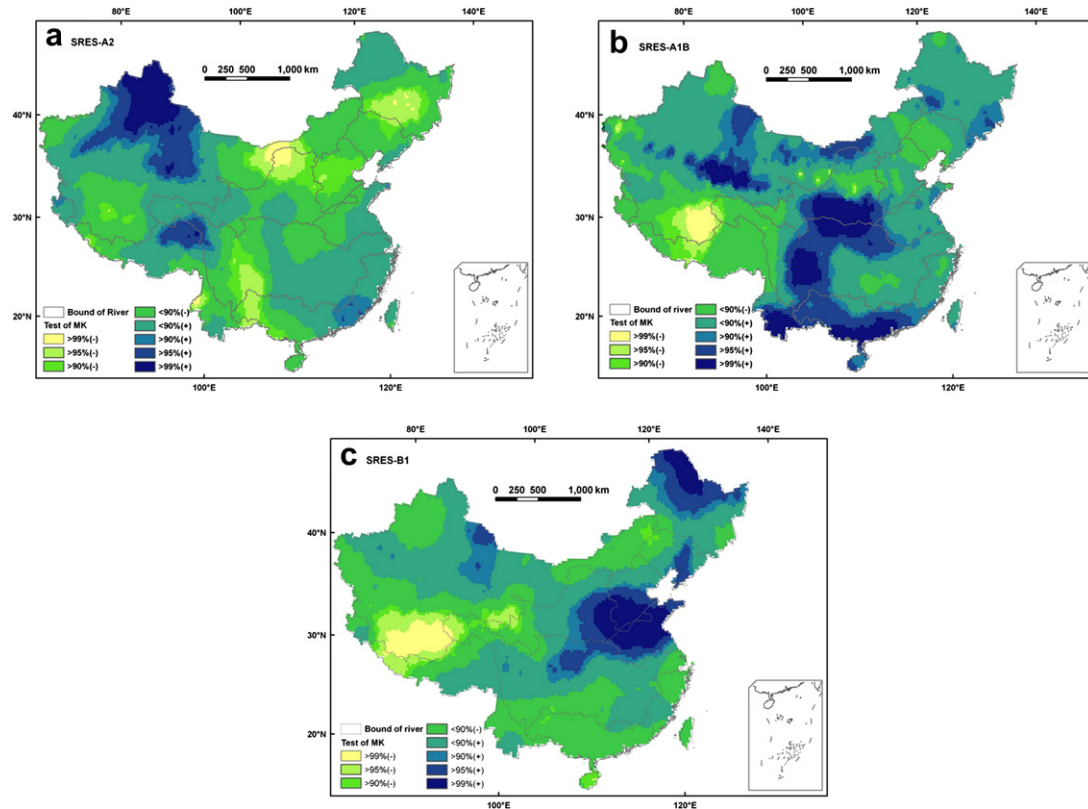


Fig. 5. Spatial distribution of the trend of dryness/wetness in China during 2002–2050.

variation of A1B scenario, and it shows a different spatial distribution; the area covered by a negative trend is greatly reduced. The trend towards drier conditions only occurs in the Liaohe River basin, the river source region of the Yellow River and the Yangtze River, and the central Qinghai-Tibet Plateau which covers the Southwest River basins and part of Northwest River basins. In some regions of the Dongting lake catchment and the Yangtze estuary, a negative trend can be detected. The trend of SPI in scenario B1 has shown a similar spatial distribution pattern with those of scenario A1B, as is illustrated in Fig. 5c. The areas showing significant trends towards drier conditions are still located in northwest China and the upper reaches of the Yellow River, the Yangtze River and the Southwest Rivers. The main difference between Fig. 5b and c is that the most parts of south China show an obvious trend towards drier conditions in scenario B1.

4.3. Change of dryness/wetness in all large river basins

Basin-averaged SPI is calculated and their trends are tested by the Mann–Kendall non-parametric method. Table 4 shows that only in the Haihe River basin a significant trend towards drier conditions can be detected, which pass the 95% confidence level in

the A2 scenario. The trend towards wetter conditions passed the 90% confidence level in the Yellow River basin (99% confidence level), the Huaihe River basin, the Yangtze River basin (95% confidence level) and the Pearl River basin (99% confidence level) in scenario A1B. Similar trends towards wetter conditions occur in the Songhuajiang River basin, the Haihe River basin, the Yellow River basin and the Huaihe River basin in scenario B1 (Table 2).

Based on monthly averaged basin-wide SPIs (Figs. 6–8), in scenario A2, there are three stages in the Songhuajiang River basin during 2002–2050 (Fig. 6a): a trend towards wetter conditions during 2002–2022; a trend towards drier conditions during 2022–2040; another wetness stage from 2040 to 2050. A period with slowly increasing wetter conditions exists in the Liaohe River basin during 2002–2022; the period from 2022 to 2038 is a dryness stage; a drying period begins in 2040 and ends in 2048 (Fig. 6b). In the Haihe River basin, there is a 10-year period with conditions alternating between dryness and wetness (Fig. 6c). There is a dry period from 2022 to 2040 in the Yellow River basin (Fig. 6d). A very similar dryness period in south China including the Huaihe River basin, the Yangtze River basin, the Pearl River basin and the Southeast River basins is projected in the 2010s, 2020s, 2030s (Fig. 6e–h). A wet period begins from 2030 in the Southwest River

Table 4
Trend of dryness in ten large river basins of China during 2002–2050.

Scenarios	Songhuajiang River basin	Liaohe River basin	Haihe River basin	Yellow River basin	Huaihe River basin	Yangtze River basin	Pearl River basin	Southeast River basins	Southwest River basins	Northwest River basins
A2	–0.33	–0.84	–1.83**	–0.45	0.12	0.24	–0.21	0.69	0.97	0.78
A1B	1.07	0.98	0.36	2.6***	1.29*	1.84**	2.62***	0.78	–0.34	0.72
B1	1.5*	0.53	1.79**	1.29*	2.64***	0.36	–0.59	–0.55	–0.41	–0.38

***Passes 99% confidence level; ** Passes 95% and * Passes 90% confidence level.

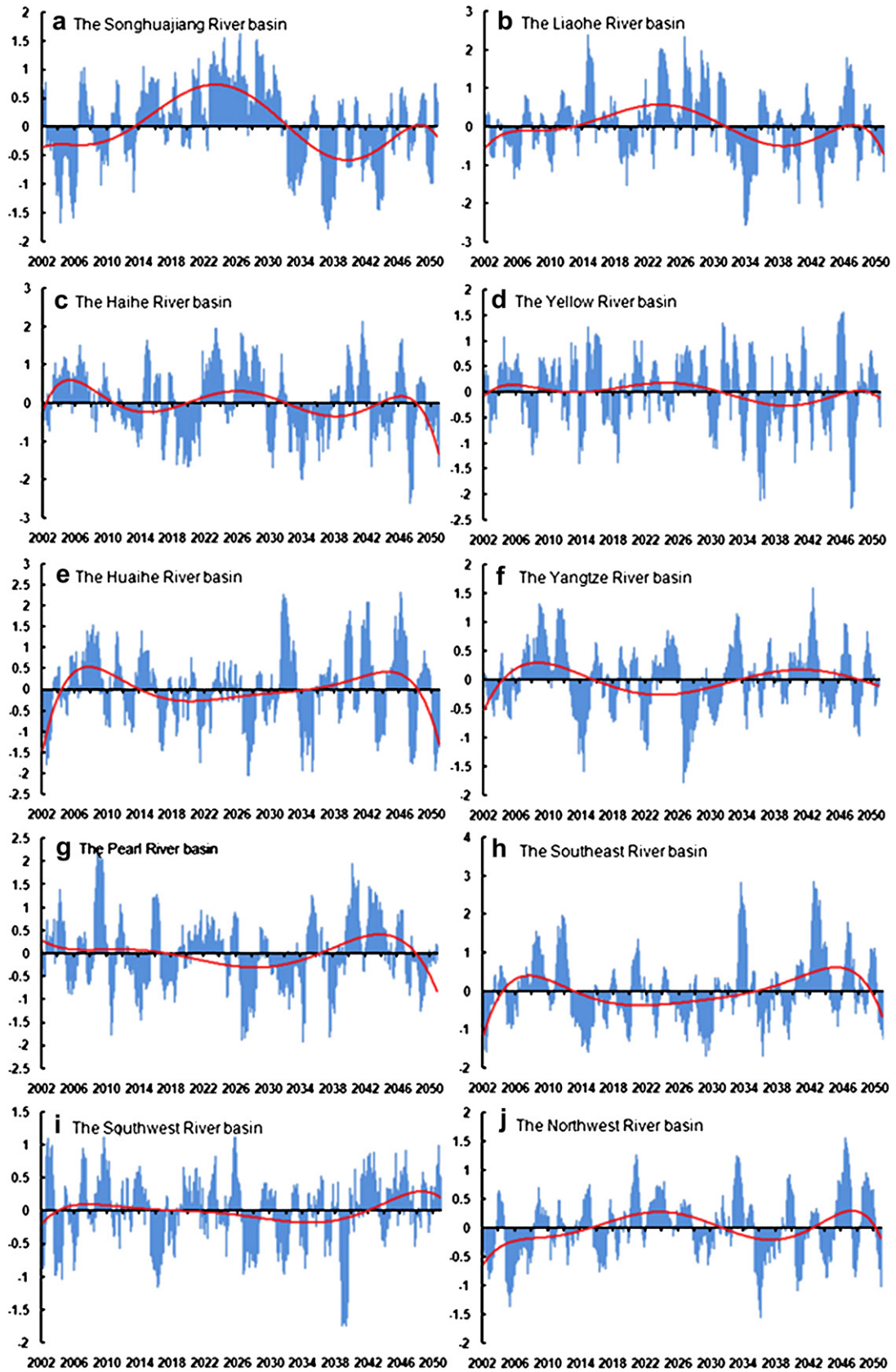


Fig. 6. Variation of SPI in ten large river basins of China during 2002–2050 in scenario A2. (Letters denote the ten river basins: a, the Songhuajiang River basin; b, the Liaohe River basin; c, the Haihe River basin; d, the Yellow River basin; e, the Huaihe River basin; f, the Yangtze River basin; g, the Pearl River basin; h, the Southeast River basins; i, the Southwest River basins; j, the Northwest Inland River basins. Letter denotation the same below.)

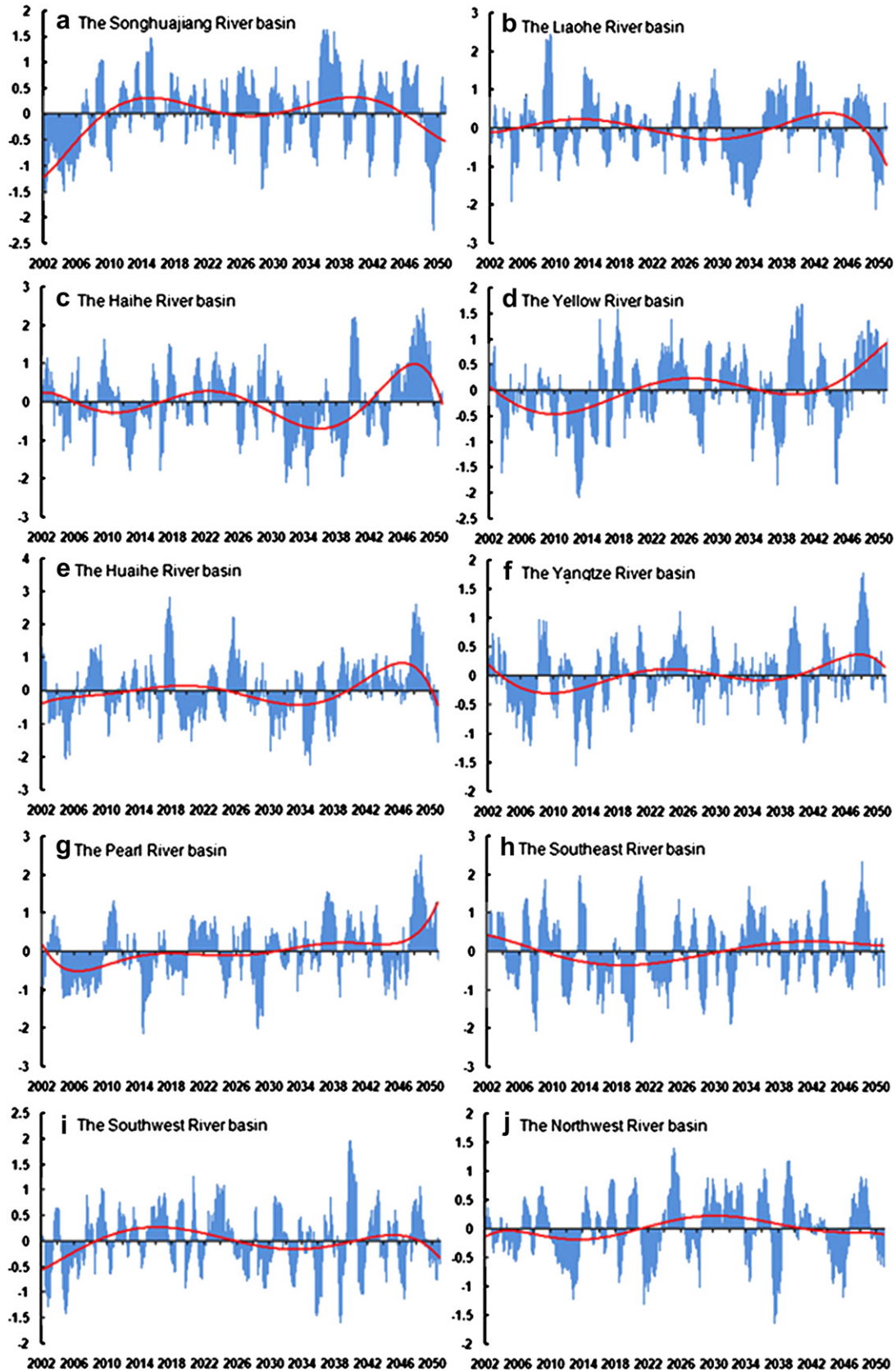


Fig. 7. Variation of SPI in ten large river basins of China during 2002–2050 in scenario A1B.

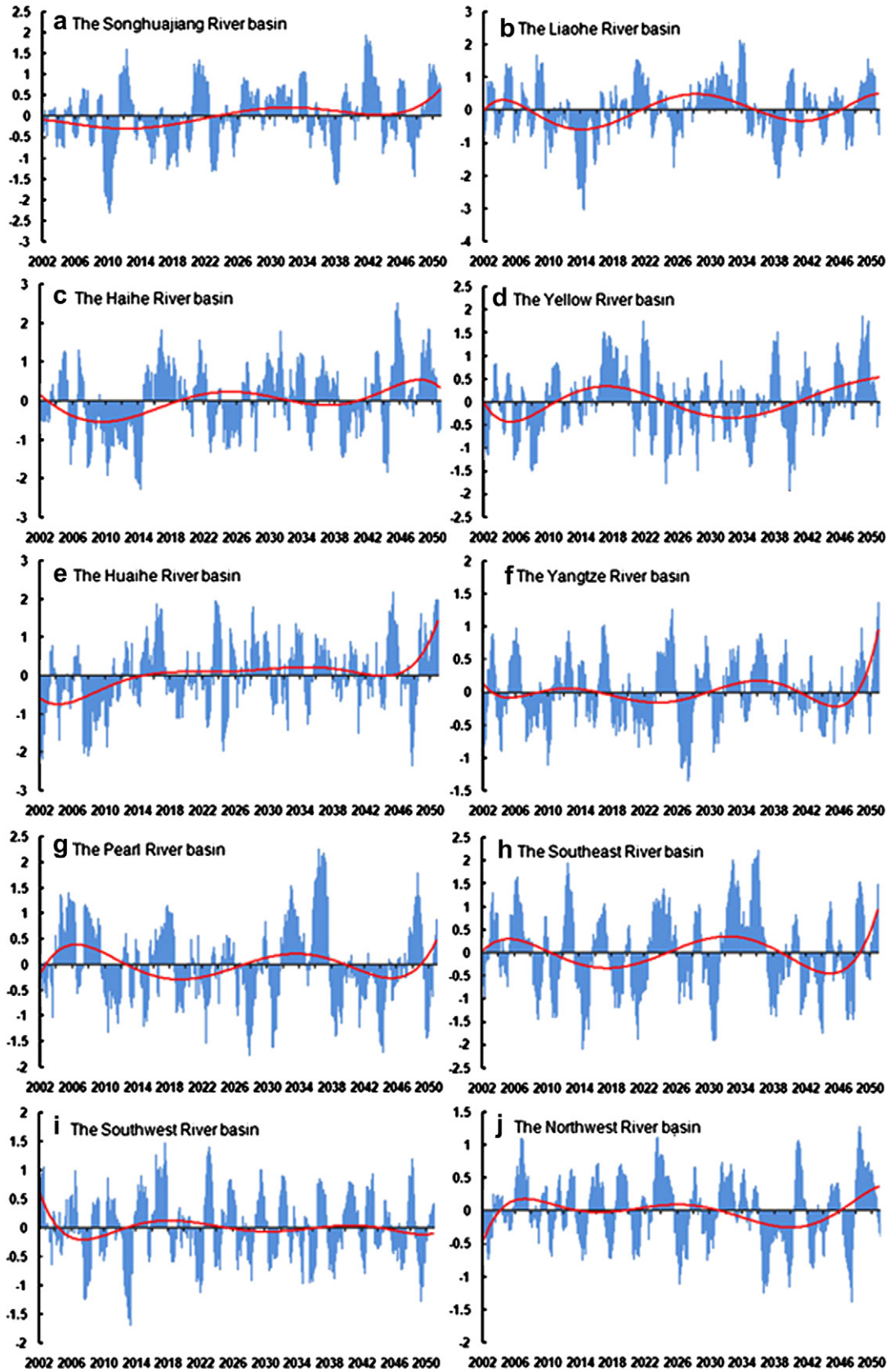


Fig. 8. Variation of SPI in ten large river basins of China during 2002–2050 in scenario B1.

Table 5a

Frequency of dry months for 10-year periods (in %) according to the SPI in ten large river basins in China during 2002–2050 (A2 scenario).

No.	River basins	2002–2010	2011–2020	2021–2030	2031–2040	2041–2050
1	Songhuajiang	76.4	15.8	23.4	22.5	42
2	Liaohe	15.3	10.9	9.9	28.7	16.6
3	Haihe	9.3	17.3	9.9	36.8	8.3
4	Yellow	17.5	27.4	10.4	15.3	13.2
5	Huaihe	19.7	18.0	11.2	25.2	5.3
6	Yangtze	19.8	21.2	12.9	15.3	12.9
7	Pearl	26.0	22.3	16.1	9.5	11.4
8	Southeast	9.2	29.8	18.6	9.3	11.5
9	Southwest	21.7	9.7	14.4	20.8	19.5
10	Northwest	13.7	18.3	16.1	15.4	17.9

basin (Fig. 6i), and a less intense wet period before 2030 in the Northwest River basin (Fig. 6j).

Fig. 7 shows the change of dryness/wetness in ten large river basins in the scenario A1B. There are not obviously changes of dryness/wetness in almost every river basin. In the 2030s and the 2040s, a dryness stage exists in the Haihe River basin (Fig. 7c). In the Yellow River basin, there is a dryness period from 2002 to 2020 (Fig. 7d). There is a dry period in the Huaihe River basin in the 2030s (Fig. 7e). In the Pearl River basin is a dry period (Fig. 7g).

Fig. 8 indicates the change rules of dryness/wetness in ten large river basins in the scenario B1. An obvious dry period occurs in the Songhuajiang River basin and the Liaohe River basin in the 2010s (Fig. 8a and b), and in the Haihe River basin during 2006–2012 (Fig. 8c), the Yellow River basin in the 2020s, and the 2030s (Fig. 8d), and in the Pearl River basin in the 2020s, and the 2040s (Fig. 8g).

The frequency of dry months according to SPI was calculated for 10-year time slices for ten large river basins under the three scenarios (Table 5). The same result can be found in Table 5 as in Figs. 6–8. In scenario A2, the frequency of dryness in northern China received its lowest value in 2030s, 4.4% in the Songhuajiang River basin, 2.9% in the Liaohe River basin, 11.9% in the Yellow River basin, and 9.9% in the Northwest River basins. Other river basins in Southern China almost reach high frequencies of dryness during 2021–2040: the Huaihe, Yangtze, Pearl, Southeast and Southwest River basins (Table 5a). In scenario A1B, the frequency of dryness is higher in the first and the last 10 years during 2002–2050. There is a downward trend in dryness frequency during 2002–2030 in the Liaohe River basin. The Haihe River basin has frequent dry months in the period 2011–2020 and 2031–2040. There is a shortage of dry months during 2021–2030 in the Yellow River basin. A downward trend but high frequency is projected in the last 10 years in the Huaihe River basin. Similarly, dry frequency during 2002–2050 is projected in the Yangtze River basin and Northwest River basins. There are downward trends of dry frequency in the Pearl and Southeast River basins (Table 5b). In scenario B1, the frequency of

Table 5b

Frequency of dry months for 10-year periods (in %) according to the SPI in ten large river basins in China during 2002–2050 (A1B scenario).

No.	River basins	2002–2010	2011–2020	2021–2030	2031–2040	2041–2050
1	Songhuajiang	48.8	20.1	4.4	58.8	41.7
2	Liaohe	16.0	8.0	2.9	32.0	21.3
3	Haihe	2.7	24.0	10.0	22.6	20.2
4	Yellow	12.8	14.7	11.9	23.4	17.2
5	Huaihe	13.5	10.3	20.0	14.9	23.9
6	Yangtze	13.0	16.7	24.6	13.0	14.2
7	Pearl	12.2	17.6	16.5	22.1	10.5
8	Southeast	9.4	21.6	23.7	11.8	6.1
9	Southwest	16.4	14.2	15.4	22.9	7.9
10	Northwest	23.9	13.8	9.9	20.5	13.9

Table 5c

Frequency of dry months for 10-year periods (in %) according to the SPI in ten large river basins in China during 2002–2050 (B1 scenario).

No.	River basins	2002–2010	2011–2020	2021–2030	2031–2040	2041–2050
1	Songhuajiang	57.3	36.8	21.6	25	22.3
2	Liaohe	12.0	24.1	8.8	19.2	10.9
3	Haihe	26.6	20.5	16.2	14.6	11.4
4	Yellow	24.7	7.1	20.5	21.3	8.4
5	Huaihe	37.3	8.5	12.3	7.1	9.8
6	Yangtze	19.3	11.9	21.4	13.8	14.8
7	Pearl	10.7	16.8	22.2	10.8	18.0
8	Southeast	13.3	23.6	18.0	10.8	20.8
9	Southwest	13.5	16.4	17.9	12.4	15.8
10	Northwest	12.9	14.4	19.1	17.9	15.1

dry months shows decreased trends in the Songhuajiang, Liaohe, Haihe, Yellow and Huaihe River basins while it shows an increased trend in Southern China (Table 5c).

5. Summary and conclusions

Drought exerts tremendous influences on agriculture and human society. Characteristics of dryness/wetness in three scenarios (A2, A1B and B1) were analyzed in this study based on the SPI, which was calculated based on the monthly precipitation data derived from ECHAM5/MPI-OM. Some results are summarized as follows.

The areas with high frequency of drought differ for the three scenarios in China during 2002–2050. In A2 scenario, an arid zone exists in north China including the Songhuajiang River basin, the Liaohe River basin, the north of the Yellow River basin and most parts of the Northwest River basins. High values were also found in the Huaihe River basin, the Jinshajiang River catchment and the Hanjiang River catchment of the Yangtze River basin and the Pearl River basin. In the A1B scenario, high value regions with over 100 dry months are located in the Songhuajiang River basin, the south of the Yellow River basin, the upper river of the Yangtze River and the Southwest River basins. However, the Haihe River basin, the east parts of the Yellow River basin, and the Southeast River basin show a high frequency of droughts.

A negative trend (trend towards drier conditions) was found from northeast to southwest of China including the Songhuajiang River basin, the Liaohe River basin, the Haihe River basin, the Yellow River basin, the upper reach of the Yangtze River, and the west part of the Pearl River basin in the A2 scenario. In the A1B scenario, a negative trend only exists in the Liaohe River basin, the Southwest River basins and in the south part of the Northwest River basins. A similar spatial distribution pattern is found in the B1 scenario. The main difference is that a trend towards drier conditions occurs in most parts of South China.

The basin-averaged SPI and frequency of drought in every basin indicate a complex future situation, in ten large river basins and specific analysis should be conducted in future research. There are many uncertainties in prediction of climate change in the future; one of reason is that Global Climate Model has limitations itself. Another is the uncertainty of regional predictions based on the results which come from the Global-scale Model. More attention should be given about the uncertainty when applying these conclusions.

Acknowledgments

The work is financially supported by the National Science Foundation of China (project no. 40601017, 40771040, 40701028). Mutual visits of the partners have been sponsored by the Sino-

German Center for Research Promotion (GZ 412). The authors are very grateful to these institutions for their financial support. Moreover, the authors express their thanks to the National Climate Center (NCC) of China Meteorological Administration (CMA) and the Potsdam Institute for Climate Impact Research for providing software to calculating SPI. Special appreciation is also given to the reviewers for their constructive suggestions.

References

- Bordi, I., Frigio, S., Parenti, P., Speranza, A., Sutera, A., 2001. The analysis of the standardized precipitation index in the Mediterranean area: regional patterns. *Annali di Geofisica* 44, 979–993.
- Bordi, I., Sutera, A., 2002. An analysis of drought in Italy in the last fifty years. *IL Nuovo Cimento* 25C, 185–206.
- Bordi, I., Fraedrich, K., Jiang, J.M., Sutera, A., 2004. Spatio-temporal variability of dry and wet periods in eastern China. *Theoretical and Applied Climatology* 79, 81–91.
- Blender, R., Fraedrich, K., 2006. Long-term memory of the hydrological cycle and river runoffs in China in a high-resolution climate model. *International Journal of Climatology* 26, 1547–1565.
- Barbosa, P., Kurnik, B., Vogt, J., Gadain, H., 2009. Using the standardized precipitation index (SPI) for drought monitoring over Africa. *Geophysical Research Abstracts* 11 EGU2009-7843.
- Dracup, J.A., Lee, K.S., Paulson, E.G.J., 1980. On the definition of drought. *Water Resources Research* 16 (2), 297–302.
- IPCC: Climate Change 2001: Synthesis Report, 2001 WG1 technical summary, 62–63. Online available at: <http://www.ipcc.ch/ipccreports/climate-changes-2001-syr-languages.htm>.
- IPCC: Climate Change 2007: the AR4 Synthesis Report, 2007. IPCC, Geneva, Switzerland. Online available at: <http://www.ipcc.ch/>.
- Kendall, M.G., 1975. Rank Correlation Methods. Charles Griffin, London, 202 pp.
- Krysanova, V., Vetter, T., Hattermann, F., 2008. Detection of change in drought frequency in the Elbe basin: comparison of three methods. *Hydrological Sciences* 53 (3), 519–537.
- Li, K.R., Yin, S.M., Sha, W.Y., 1996. Characteristics of time–space of recent drought in China. *Geographical Research* 15 (3), 6–15.
- Li, X.Z., Liu, X.D., Ma, Z.G., 2004. Analysis on the drought characteristics in the main arid regions in the world since recent hundred-odd years. *Arid Zone Research* 21 (2), 97–103.
- Mann, H.B., 1945. Non-parametric test against trend. *Econometrica* 13, 245–259.
- McKee, T.B., Doesken, N.J., Kleist, J., 1993. The relationship of drought frequency and duration to time scales. In: Eighth Conference on Applied Climatology, January 17–22.
- Moreira, E.E., Paulo, A.A., Pereira, L.S., Mexia, J.T., 2006. Analysis of SPI drought class transitions using loglinear models. *Journal of Hydrology* 331, 349–359.
- Moreira, E.E., Coelho, C.A., Paulo, A.A., Pereira, L.S., Mexia, J.T., 2008. SPI-based drought category prediction using loglinear models. *Journal of Hydrology* 354, 116–130.
- Ma, Z.G., Ren, X.B., 2007. Drying trend over China from 1951 to 2006. *Advances in Climate Change Research* 3 (4), 195–201.
- Narasimhan, B., Srinivasan, R., 2005. Development and evaluation of soil moisture deficit index (SMDI) and evapotranspiration deficit index (ETDI) for agricultural drought monitoring. *Agricultural and Forest Meteorology* 133, 69–88.
- Nakicenovic, N., Swart, R., 2000. Special Report on Emissions Scenarios. Cambridge University Press, Cambridge, 599 pp.
- Paulo, A.A., Pereira, L.S., Matias, P.G., 2003. Analysis of local and regional droughts in southern Portugal using the theory of runs and the standardized precipitation index. In: Rossi, G., Cancelliere, A., Pereira, L.S., Oweis, T., Shatanawi, M., Zairi, A. (Eds.), *Tools for Drought Mitigation in Mediterranean Regions*. Kluwer, Dordrecht, pp. 55–78.
- Raziei, T., Saghafian, B., Paulo, A.A., Pereira, L.S., Bordi, I., 2009. Spatial patterns and temporal variability of drought in Western Iran. *Water Resources Management* 23, 439–455.
- Su, B.D., Gemmer, M., Jiang, T., Ren, G.Y., 2007. Probability distribution of precipitation extremes over the Yangtze River basin during 1960–2005. *Advances in Climate Change Research* 3 (4), 208–213.
- Sun, Y., Ding, Y.H., 2008. Validation of IPCC AR4 climate models in simulating interdecadal change of East Asian summer monsoon. *Acta Meteorologica Sinica* 66 (5), 765–780.
- Tsakiris, G., Vangelis, H., 2004. Towards a drought watch system based on spatial SPI. *Water Resources Management* 18, 1–12.
- von Storch, H., Zwiers, F.W., 1999. *Statistical Analysis in Climate Research*. Cambridge University Press, Cambridge.
- Wilks, D.S., 1995. *Statistical Methods in the Atmospheric Sciences*. Academic Press.
- Wang, Z.W., Zhai, P.M., 2003. Climate change in drought over Northern China during 1950–2000. *Acta Geographica Sinica* 58 (Suppl.), 61–68.
- Wei, F.Y., 2004. Characterization of drought strength in North China and its climatic variation. *Journal of Natural Disasters* 13 (2), 32–38.
- Xie, A., Sun, Y.G., Bai, R.H., 2003. Arid climate trend over Northeastern China and its response to global warming. *Acta Geographica Sinica* 58 (Suppl.), 75–82.
- Zhang, Q., 1998. Research on determination of drought index in North China and its application. *Journal of Catastrophology* 13 (4), 34–38.
- Zhang, Q., Jiang, T., Gemmer, M., Becker, S., 2005. Precipitation, temperature and runoff analysis from 1950 to 2002 in the Yangtze basin, China. *Hydrological Sciences* 50 (1), 65–80.
- Zhai, P.M., Zou, X.K., 2005. Changes in temperature and precipitation and their impacts on drought in China during 1951–2003. *Advances in Climate Change Research* 1 (1), 16–18.